

1 **Separable systems for recovery of finger strength and control after stroke**

2 **Running title: post-stroke recovery of hand function**

3
4 Jing Xu^{1*}, Naveed Ejaz^{2,3*}, Benjamin Hertler⁴, Meret Branscheidt^{4,7}, Mario Widmer⁴,
5 Andreia V. Faria⁵, Michelle D. Harran⁶, Juan C. Cortes⁶, Nathan Kim¹, Pablo A. Celnik⁷,
6 Tomoko Kitago⁶, Andreas R. Luft^{4,8}, John W. Krakauer¹, Jörn Diedrichsen^{2,3}

7
8 1. Department of Neurology and Neurosciences, Johns Hopkins University, Baltimore,
9 MD, USA

10 2. Institute of Cognitive Neuroscience, University College London, London, UK

11 3. Brain Mind Institute, Western University, London, ON, Canada

12 4. Division of Vascular Neurology and Rehabilitation, Department of Neurology,
13 University Hospital and University of Zürich, Zürich, Switzerland

14 5. Department of Radiology, Johns Hopkins University, Baltimore, MD, USA

15 6. Department of Neurology, Columbia University, New York, NY, USA

16 7. Department of Physical Medicine and Rehabilitation, Johns Hopkins University,
17 Baltimore, MD, USA

18 8. Cereneo Center for Neurology and Rehabilitation, Vitznau, Switzerland

19
20 **Author Contributions**

21 * These authors contributed equally to this work

22 J.X., J.W.K., and J.D. designed the experiment. The data were collected by J.X., B.H.,

23 M.B., M.W., M.H., J.C.C., and N.K.. Data collection from each site was directed by

24 J.W.K., P.A.C., T.K., and A.R.L.. Data analyses were conducted by J.X., N.E., A.F., and
25 J.D. The article was written by J.X., J.W.K., N.E., and J.D..

26

27 **Correspondence**

28 Jing Xu

29 Department of Neurology

30 School of Medicine

31 Johns Hopkins University

32 Pathology 2-210

33 600 N. Wolfe St.

34 Baltimore, MD 21287 USA

35 Tel: (410) 955-9314

36 Email: jing.xu@jhmi.edu

37

38 **Number of words:**

39 Title: 74 chars (limit 160)

40 Abstract: 151 words (limit 250)

41 New & Noteworthy: 70 words (limit 75)

Abstract

42

43 Impaired hand function after stroke is a major cause of long-term disability. We
44 developed a novel paradigm that quantifies two critical aspects of hand function, strength
45 and independent control of fingers (individuation), and also removes any obligate
46 dependence between them. Hand recovery was tracked in 54 patients with hemiparesis
47 over the first year after stroke. Most recovery of strength and individuation occurred
48 within the first three months. A novel time-invariant recovery function was identified:
49 recovery of strength and individuation were tightly correlated up to a strength level of
50 approximately 60% of estimated premorbid strength; beyond this threshold, strength
51 improvement was not accompanied by further improvement in individuation. Any
52 additional improvement in individuation was attributable instead to a second process that
53 superimposed on the recovery function. We conclude that two separate systems are
54 responsible for post-stroke hand recovery: one contributes almost all of strength and
55 some individuation; the other contributes additional individuation.

56

New & Noteworthy

57 We tracked recovery of the hand over a one-year period after stroke in a large cohort of
58 patients, using a novel paradigm that enabled independent measurement of finger strength
59 and control. Most recovery of strength and control occurs in the first 3 months after
60 stroke. We found that two separable systems are responsible for motor recovery of hand:
61 one contributes strength and some dexterity, whereas a second contributes additional
62 dexterity.

63

64

Keywords

65 finger individuation, strength, stroke, motor recovery, plasticity

66 The human hand possesses a large repertoire of movements. Two critical aspects
67 span its functional space: *strength*, as manifest in a power grip, and *control* of individual
68 finger movements, as in piano playing (Napier 1956; Connolly and Elliott 1972). The
69 most common observation after stroke is that both are impaired (Kamper and Rymer
70 2001; Lang and Schieber 2003). Weakness in both finger flexion and extension leads to
71 difficulties in producing a strong grip and opening the hand (Colebatch and Gandevia
72 1989; Kamper et al. 2003). Loss of finger control manifests as inability either moving a
73 single finger while keeping the others immobile, or making complex hand gestures, both
74 of which impair the ability to perform tasks such as typing or buttoning a shirt (Kamper
75 and Rymer 2001; Li et al. 2003; Lang and Schieber 2004). When strength does recover
76 after stroke, control often remains impaired, causing lasting disability (Heller et al. 1987;
77 Sunderland et al. 1989). However, the relationship between strength and control after
78 stroke remains poorly understood. Separating the effect of stroke on finger strength
79 versus control is a challenge given that most current clinical measurements cannot
80 adequately separate weakness from deficits in control. In the current study we therefore
81 sought to develop a new paradigm that could measure these two aspects of hand function
82 separately, and to investigate the relationship between strength and control over the time
83 course of hand recovery after stroke. We were specifically interested in testing whether
84 these two components recover in a lawful relationship with each other, or whether they
85 recover independently.

86 To isolate these two aspects of hand function, it is necessary to remove any
87 obligatory relationship between them (Reinkensmeyer et al. 1992), i.e. derive a control
88 measure that is independent of strength. Intuitively, a rock climber may have stronger

89 fingers than a pianist, but not necessarily superior control of individual fingers. Schieber
90 (Schieber 1991) devised an individuation task requiring participants to move individual
91 fingers while attempting to keep the non-moving ones stationary. Movements of the
92 uninstructed fingers were used as a measure of loss of control. This paradigm, however,
93 does not assess the relationship between forces that patients can generate and
94 individuation ability. In the paradigm used here, we first measured the maximum
95 voluntary contraction force (MVF) that participants could produce with each finger. We
96 then asked participants to produce isometric forces over four sub-maximal levels with
97 each finger, while trying to keep the uninstructed fingers immobile. Even healthy people
98 show involuntary force production (enslaving) on the uninstructed fingers, which
99 increases with the required instructed finger force level (Li et al. 1998; Zatsiorsky et al.
100 2000). The slope of the function of uninstructed finger enslaving on instructed finger
101 force thus provides a measure of individuation that is independent of strength.

102 Using this paradigm we tracked the recovery of hand strength and finger
103 individuation in patients over a one-year period after stroke. One possibility is that
104 strength and control recover independently. For example, a patient may remain quite
105 weak but have good recovery of individuation, or a patient may recover a significant
106 amount of grip strength but fail to individuate the digits. Alternatively, recovery may be
107 such that when strength recovers so does individuation, because either they share a
108 common neural substrate, or biological repair processes proceed at similar rates in
109 separate neural substrates. Using fine-grained behavioral analysis, we show that the
110 recovery of strength and individuation is mediated by two separable systems: one
111 contributes mainly strength but also some individuation, whereas the other contributes

112 additional individuation. Lesion analysis provided a clue as to what the anatomical basis
113 for this separation might be.

114

115 **Materials and Methods**

116 *Participants*

117 Fifty-four patients with first-time ischemic stroke and hemiparesis (34 male, 20
118 female; mean age 57.4 ± 14.9 years) were recruited from three centers: The Johns Hopkins
119 Hospital and Affiliates, Columbia University Medical Center, and The University
120 Hospital of Zurich and Cereneo Center for Neurology and Rehabilitation. According to
121 the Edinburgh Handedness Inventory (Oldfield 1971), forty-four patients were right- and
122 10 were left-handed. All patients met the following inclusion criteria: 1) First-ever
123 clinical ischemic stroke with a positive DWI lesion within the previous 2 weeks; 2) One-
124 sided upper extremity weakness (MRC < 5); 3) Ability to give informed consent and
125 understand the tasks involved. We excluded patients with one or more of the following
126 criteria: initial upper extremity Fugl-Meyer Assessment (UE FMA) $> 63/66$ (Fugl-Meyer
127 et al. 1975), age under 21 years, hemorrhagic stroke, space-occupying hemorrhagic
128 transformation, bihemispheric stroke, traumatic brain injury, encephalopathy due to
129 major non-stroke medical illness, global inattention, large visual field cut (greater than
130 quadrantanopia), receptive aphasia (inability to follow 3-step commands), inability to
131 give informed consent, major neurological or psychiatric illness that could confound
132 performance/recovery, or a physical or other neurological condition that would interfere
133 with arm, wrist, or hand function recovery. Due to the exclusion of aphasic patients, the
134 sample had a bias towards right-sided infarcts (17 left-sided, 37 right-sided). The lesion

135 distribution is shown in Fig. 5a. Of the 54 patients, 21 were on fluoxetine or other types
136 of serotonin reuptake inhibitors (SRI) over the course of the study. For detailed patient
137 characteristics, see Table 1.

138 We also recruited 14 age-matched healthy control participants (10 male, 4
139 female; mean age 64 ± 8.2 years; all right-handed) at the three centers. There was no age
140 difference between patient and control samples (two-samples t-test $t(65) = 1.60$, $p =$
141 0.11), nor did the ratio of gender and handedness in the two groups differ (Fisher's exact
142 test $p = 0.11$ and 0.75 , respectively). The healthy controls did not have any neurological
143 disorder or physical deficit involving the upper limbs. All participants signed a written
144 consent, and all procedures were approved by Institutional Research Board at each study
145 center.

146 -----
147 Insert Table 1
148 -----

149 ***Assessment of finger maximum voluntary contraction and of individuation***

150 To achieve good characterization of hand function recovery, the study design
151 required patient testing at the following five time points post-stroke: within the first 2
152 weeks (W1, 10 ± 4 days), at 4-6 weeks (W4, 37 ± 8 days), 12-14 weeks (W12, 95 ± 10 days),
153 24-26 weeks (W24, 187 ± 12 days), and 52-54 weeks (W52, 370 ± 9 days). Healthy controls
154 were tested at comparable intervals.

155 At each of the five visits, hand function was tested using an ergonomic device that
156 measures isometric forces produced by each finger (Fig. 1a). The hand-shaped keyboard
157 was comprised of ten keys. Force transducers (FSG-15N1A, Honeywell®; dynamic range

158 0-50 N) measured the downward flexion force exerted at each fingertip with a sampling
159 rate of 200 Hz. The data were digitized using National Instrument USB-621x devices
160 interfacing with MATLAB (The MathWorks, Inc., Natick, MA) Data Acquisition
161 Toolbox. Visual stimuli were presented on a computer monitor, run by custom software
162 written in MATLAB environment using the Psychophysics Toolbox (Psychtoolbox)
163 (Brainard 1997).

164 Participants were seated in a comfortable chair, facing the computer monitor.
165 Throughout the experiment, participants rested their two hands on the keyboards with
166 each finger on top of a key, their wrists strapped and fixed on a wrist-rest, with forearms
167 extended and supported by foam arm rests. Ten vertical gray bars representing the ten
168 digits were shown at the top of the screen, and another ten vertical bars below them
169 instructed the amount of force to be exerted; the required force level for each finger per
170 trial was indicated by the height of a green section within one of the vertical gray bars
171 (Fig. 1b). Participants could monitor the force exerted by all ten fingers in real time by
172 the heights of ten small white horizontal lines moving along the vertical force bars.

173 Two separate aspects of finger function were tested: maximal voluntary
174 contraction force (MVF) and individuation. During each MVF trial, participants were
175 asked to depress one finger at a time with maximum strength, and to maintain this force
176 level for two seconds. The participants could press with the other fingers as much as they
177 wanted as long as maximal force on the instructed finger was achieved. To signal the
178 start, one force bar corresponding to the instructed finger turned green. MVF was
179 measured twice per finger.

180 In each individuation trial, participants had to press only one finger at a sub-MVF
181 force level, while at the same time keeping other fingers immobile on the keys. Four
182 target force levels were tested for each digit: 20%, 40%, 60%, and 80% of MVF; each
183 level was repeated 4 times. On each trial, the participant was asked to bring the
184 corresponding white line up to the force target line (black line in the middle of green
185 region, representing the 25% upper and lower bounds of target force level) (Fig. 1b), and
186 maintain the force level for 0.5 sec. If no response passing the force threshold of 2.5N
187 was detected within two seconds, the trial was terminated.

188 -----
189 Insert Figure 1
190 -----

191 ***Clinical assessments***

192 At each visit, all participants were also assessed with several clinical outcome
193 measures. Here we report data for FMA, Action Research Arm Test (ARAT) (Lyle
194 1981). UE FMA, a clinical measure of motor impairment (WHO, 2002), was graded by a
195 trained assessor using the UE Fugl-Meyer (FM) scale, where a higher score connotes
196 lower impairment (Fugl-Meyer et al., 1975). We summarized subscores for the entire
197 upper extremity (FM-Arm, maximum 66) and hand (FM-Hand; maximum 14).

198 ***Data analysis***

199 *Strength Index.* The 95th percentile of the force traces produced across all
200 sampled force data points during the finger depressing period in each trial was calculated,
201 and then averaged across the two MVF trials to obtain a measure of MVF for each digit.
202 If the force achieved on one of the two trials was below 60% of that produced on the

203 other trial, only the larger force was taken as the MVF measure (6.5% of trials were
 204 excluded). The overall strength of the hand was then calculated by averaging across all
 205 five digits. To account for large inter-subject variability in premorbid strength, all MVF
 206 values were normalized by MVF of the non-paretic hand at W52, estimated using a
 207 mixed-effects model (see below). This normalization provided a Strength Index, with a
 208 value close to 1 implying full recovery. For control participants, one hand was randomly
 209 assigned as the “nonparetic” hand for normalization purposes. To account for possible
 210 laterality effects, the assignment followed the ratio of dominant to non-dominant hands
 211 found in the patients (~10:4).

212 *Individuation Index.* If individuation were perfect, a participant should be able to
 213 press the instructed finger without any force being exerted by the uninstructed fingers.
 214 For each time bin t (5ms) in a single trial, the enslaved deviation of the force of each
 215 uninstructed finger ($F_{t,j}$) from baseline force (BF_j) was calculated, assessed at the
 216 beginning of the trial when a go cue was presented. This deviation was averaged over all
 217 bins (T) in the force trace from the go cue to the end of the trial:

$$218 \quad \text{meanDevP} = \frac{1}{T} \sum_{t=0}^T \sqrt{\sum_{j=\text{passive}} (F_{t,j} - BF_j)^2} \quad (1)$$

219 where index j denotes the j th uninstructed finger. A higher *mean deviation* indicates more
 220 enslaving of the uninstructed finger.

221 For a measure of individuation ability, it is necessary to account for the
 222 relationship between force deviations of the uninstructed fingers and the force produced
 223 by the instructed finger. Consistent with previous reports (Li et al. 1998), we observed
 224 that enslaving of uninstructed fingers increases with higher instructed finger force (Fig.

225 1e, h). The relationship between the two variables was close to linear. Thus, a good
226 measure of individuation reflects how much the mean deviation in uninstructed fingers
227 increases for each N of force produced by the instructed finger. The ratio of these two
228 variables can be reliably estimated by fitting a regression line without an intercept. To
229 reduce the influence of outliers, we used robust regression (Holland and Welsch 1977).
230 The *slope* of the regression line reflects individuation ability: smaller slope corresponds
231 to better individuation, 0 being the best case, meaning uninstructed fingers perfectly
232 immobile at any instructed finger force level. Because the regression slope is bounded by
233 zero (as mean deviation is positive), its distribution is positively skewed. To allow for the
234 use of parametric statistics, the slope was log-transformed. The sign of this value was
235 inverted so that higher values would correspond to better function. The negative log slope
236 was calculated separately for each instructed finger and then averaged across fingers. The
237 same normalization procedure as for the Strength Index was then applied to the averaged
238 negative log slope to provide the final Individuation Index.

239 *Reliability measures for Strength and Individuation.* To determine the reliability
240 of the Strength and Individuation Indices, split-half reliabilities for both measures were
241 calculated. For the Strength Index, we used one MVF trial per digit in each split. We then
242 calculated the Strength Index (normalized) on each half of the data independently in the
243 same way as for the full data set. The correlation between the two halves across all
244 available sessions and patients was then used as a measure of split-half reliability.

245 For the Individuation Index, data from each finger was split such that two trials
246 per force level were assigned to each split. The Individuation Index was then calculated
247 separately for each split from the slope of the regression line, and normalized in the same

248 way as Strength Index. We repeated the split multiple times, each time assigning trials at
249 random and then averaging the split-half correlations from all splits for more reliable
250 results.

251 Split-half correlation will underestimate reliability because the variability in each
252 half will be higher than the variability when using all the data (Guttman 1945). The
253 estimate was therefore corrected using the formula

$$254 \quad r_{full} = \frac{2r_p}{r_p + 1} \quad (1)$$

255 where r_p is the correlation between the two splits.

256 *Stability analysis.* To assess whether the relative deficits in strength and
257 individuation remained stable across different testing time points, or whether there was
258 meaningful biological change, we calculated the correlation of each measure across
259 neighboring testing time points. One caution when interpreting these correlations is that
260 the correlation between two repeated measures will always be smaller than 1 even if the
261 underlying factor did not change, because both measures contain some measurement
262 noise. To account for this effect, we used the reliability (r_{full}) of the measure at each time
263 point to compute a noise ceiling, which indicates how much two repeated noisy
264 measurements should correlate with each other if the underlying variable were perfectly
265 stable:

$$266 \quad r_{noise\ ceiling} = \sqrt{r1_{full} * r2_{full}} \quad (2)$$

267 *Statistical analysis and handling of missing data.* Data analysis was performed
268 using custom-written MATLAB and R (R Core Team, 2012) routines. The analysis

269 focused on the Strength and Individuation Indices, but was also performed on standard
270 clinical assessments, FMA and ARAT.

271 The requirement for 5 post-stroke time-points was ambitious, with the
272 consequence of some missing sessions. A total of 21 patients completed all five time-
273 points; on average each patient completed 3.6 sessions (total number of patients at each
274 time points are: 39, 39, 40, 39, and 34 for W1-52, respectively); thus a total of 75% of the
275 possible sessions were acquired. Missing sessions were treated as data missing-at-
276 random. To optimally use all the measured data, we employed linear mixed-effect
277 models. The model specifies joint distributions for observed and missing observations.
278 Parameters of those distributions can thus be estimated by maximizing the likelihood of
279 the data under the model. There are several advantages to this approach: First, all the
280 available data can be used and there is no need to exclude any data. Secondly, it avoids
281 the statistical pitfalls inherent in “filling in” missing observations with point estimates.
282 Linear mixed-effect models implemented in the *lme4* package in R (Bates et al. 2014)
283 were used to test changes in these measures over time. Participant was taken as a random
284 factor. Time Point (five time points from W1-W52) and Hand Condition (paretic, non-
285 paretic, and control) were considered fixed factor. The model was applied to control and
286 patient data separately. Mixed-effect model estimation for group summary statistics was
287 implemented in MATLAB using the restricted maximum likelihood method (Laird and
288 Ware 1982).

289 *Modeling the time-invariant function.* To test the hypothesis that there is a time-
290 invariant relationship between strength and individuation, a two-segment piecewise linear
291 function was fitted. This function had four free parameters: the intercept, the location of

292 the inflection point, and the slope on each side of the inflection point. Let x be the
 293 predictor with two segments separated by a constant breakpoint c , $x_1 \leq c$ and $x_2 \geq c$. The
 294 linear functions for each segment are

$$\begin{aligned}
 295 \quad y_{1i} &= b_{10} + b_{11}x_{1i} + e_{1i} \\
 y_{2i} &= b_{20} + b_{21}x_{2i} + e_{2i}
 \end{aligned}
 \tag{3}$$

296 The two pieces can be joined at the breakpoint constant c by setting $y_{1i} = y_{2i}$, yielding

$$\begin{aligned}
 297 \quad b_{20} &= b_{10} + (b_{11} - b_{21})c \\
 y_{2i} &= b_{10} + (b_{11} - b_{21})c + b_{21}x_{2i} + e_{2i}
 \end{aligned}
 \tag{4}$$

298 Putting the two pieces together, we have the full model

$$299 \quad y_i = a + b_1x_i \cdot I(x_i \leq c) + [(b_1 - b_2)c + b_2x_i] \cdot I(x_i \geq c) + e_i \tag{5}$$

300 where $I(\cdot)$ is an indicator variable, coded as 1's or 0's to indicate the condition satisfied.

301 The maximum-likelihood (least-squares) estimates of these parameters were
 302 obtained by using the non-linear optimization routine `fminsearch` in Matlab. This time-
 303 invariant model with fixed parameters across all time points was then compared with a
 304 more complex model that allowed free parameters for each time point, using leave-one-
 305 out cross-validation (Picard and Cook 1984) to assess whether this function changed
 306 systematically over time, or whether it was time-invariant. Cross validation provides an
 307 unbiased estimate of a model's ability to predict new data and automatically penalizes
 308 models that are too complex.

309 *Lesion Imaging and Quantification*

310 *Imaging acquisition and lesion distribution.* Images were acquired following the
 311 same testing schedule as behavior assessment, using 3T MRI Phillips scanner, and
 312 consisted of two DTI datasets (TR/TE=6600/70ms, EPI, 32 gradient directions, b=700

313 s/mm²) and an MPRAGE T1-WI (TR/TE=8/3.8ms) sequence. FOV, matrix, number of
314 slices, and slice thickness were 212×212 mm, 96×96 (zero-filled to 256x256), 60,
315 2.2mm, respectively, for DTI; and 256×256mm, 256×256, 170, 1.2mm, respectively, for
316 T1-WI. The DTI were processed using DtiStudio (www.MRISstudio.org) and the mean
317 diffusion-weighted image (DWI) was calculated.

318 To define the boundary(s) of the acute stroke lesion(s) for each participant, a
319 threshold of >30% intensity increase from the unaffected area in the first-time-point
320 diffusion-weighted image (DWI) extracted from DTI images (Leigh et al. 2013) was first
321 applied. Then a neuroradiologist (AVF), blind to the patients' clinical information,
322 manually modified the boundary to avoid false-positive and false-negative areas on the
323 RoiEditor software (www.MRISstudio.org). Following the standard in the field, the
324 definitions were double checked by a second rater (MB). The averaged lesion distribution
325 map across all patients in the current study is shown in Fig. 5a. For the seven patients
326 who had no DTI in the acute phase, lesion definition was performed on the clinical DWI,
327 which has lower resolution (1x1mm in plane, 4-6mm thickness). Analysis
328 of white matter ROIs, including the CST, was not performed in these seven patients.

329 *Region of interest definition and lesion quantification.* The focus was on two
330 ROIs: 1) The cortical gray matter of the hand area in the motor cortex; 2) The entire CST
331 superior to pyramids, identified by probabilistic maps derived from tract tracing methods
332 (see below). The *percentage-volume-affected* in these regions was computed as a ratio of
333 the number of voxels affected by the lesion divided by the total number of voxels in the
334 entire ROI. This measure was correlated with our main outcome measures, the Strength
335 and Individuation Indices.

336 To define the CST, each image and respective lesion were first mapped to a single
337 subject adult template, the JHU-MNI atlas (Mori et al. 2008; Oishi et al. 2008), using
338 affine transformation followed by dual channel (both b0 and FA maps) large deformation
339 diffeomorphic metric mapping (LDDMM) (Ceritoglu et al. 2009). This template has
340 already been segmented into more than 200 regions of interest (ROIs), and contains
341 probabilistic maps of multiple tracts, including the CST (Mori et al. 2005; Oishi et al.
342 2010; Zhang et al. 2010). To ensure accurate mapping in the lesioned areas, we first used
343 "artificial" images in which the stroke area was masked out and substituted by the normal
344 images from the contralateral hemisphere. This helped minimize inaccuracies caused by
345 focal changes in intensity due to the stroke. In addition, also to avoid inaccuracy caused
346 by lesion, we directly applied the probabilistic map of the CST to each patient's image.
347 The original probabilistic map CST was defined based on 20 healthy participants in a
348 previous study (Zhang et al. 2010), using an automated Fiber Assignment by Continuous
349 Tractography (FACT) method (Wakana et al. 2007; Zhang et al. 2008). Specifically, the
350 initial seeds were placed in the middle portion of cerebral peduncle and traced back to the
351 precentral (primary motor) cortex. Multiple reference ROIs were then placed in regions
352 along the tracts, including the pyramids, to which "NOT", "AND", "CUT", and "OR"
353 logic operations were applied, to ensure that the delineation was as consistent as possible
354 with existing anatomical knowledge of the CST. Lateral motor cortices were not included
355 because of mixing of fibers with different orientations within each pixel. The particular
356 sequence of ROIs and logic operations used to isolate the CST reflects a trade-off
357 between sensitivity and reliability, and has been shown to have high level of intra- and
358 inter-rater reproducibility (Wakana et al. 2007). The white matter tracts were identified

359 with a fractional anisotropy threshold of 0.2. The probabilistic map was then “back-
360 warped” to each patient’s individual space by a series of LDDMM mapping.

361 A different approach was used to define an ROI that would encompass the hand
362 area of the primary motor cortex. The hand ROI was defined on the average
363 reconstruction of the cortical surface available in the Freesurfer software (Dale et al.
364 1999), selecting Brodmann area (BA) 4 based on cytoarchitectonic maps (Fischl et al.
365 2008). To restrict the ROI to the area of motor cortex involved in the control of the upper
366 limb, we only included the area 2.5 cm dorsal and ventral to the hand knob (Yousry et al.
367 1997). The defined ROI was then morphed into MNI space using the surfaces of the age-
368 matched controls. These ROIs were then brought to the JHU-MNI atlas (in which each
369 subject’s image and respective stroke area were already mapped, as mentioned above)
370 using T1-based LDDMM to construct a probabilistic map of the hand area. The
371 probabilistic map was threshold of 70% to calculate percent-volume affected.

372

373

Results

374 In a large-scale longitudinal study, we tracked recovery of two behavioral
375 components of hand function: strength and finger control, using a novel paradigm that
376 measures them independently. A total of 54 patients with acute stroke and 14 healthy
377 controls were tested five times over a one-year period. Data in the final analysis
378 comprised a total of 251 sessions tested in 53 patients (one patient only completed two
379 blocks of the task, and was thus removed from further analysis) and 14 controls. Forty-
380 one patients and twelve controls completed ≥ 3 sessions. (see details in Materials and
381 Methods).

382 ***Strength and Individuation Indices were reliable.***

383 At each of the five visits, hand function was tested using an ergonomic device that
384 measures isometric forces produced by each finger (Fig. 1a). Two separate aspects of
385 finger function were tested: strength (MVF) and individuation (Fig. 1b).

386 Finger strength was assessed by measuring MVF for each finger separately and
387 then averaged across all fingers for each hand. MVF for healthy controls had an average
388 value of 20.35 N (SD = 8.56) for the dominant hand, and 22.76 N (SD = 6.89) for the
389 non-dominant hand. The normalized Strength Index (see Materials and Methods) for the
390 controls' dominant hand was 1.00 (SD = 0.19), and non-dominant hand was 1.17 (SD =
391 0.25). For patients, the mean for the non-paretic hand was 0.93 (SD = 0.20), and for the
392 parietic hand was 0.59 (SD = 0.38). For the parietic hand, Strength Indices did not
393 correlate with age ($r = 0.04$, $p = 0.75$), nor were they affected by gender ($t(51) = 0.98$, $p =$
394 0.33) or handedness ($t(51) = 0.10$, $p = 0.92$).

395 To assess individuation, we measured the amount of involuntary force changes on
396 the uninstructed fingers (enslaving (Zatsiorsky et al. 2000)) for different levels of force
397 production with the instructed fingers. The amount of enslaving systematically increased
398 at higher force levels (Fig. 1c-h). Loss of control at increasing force levels has been
399 shown for angular position of the fingers (Li et al. 1998) and reaching radius of the arm
400 after stroke (Sukal et al. 2007). To control for this relationship, we characterized the
401 Individuation Index as the slope of the function between instructed finger force and
402 uninstructed enslaving (see Materials and Methods). Lower values of Individuation Index
403 indicate more impaired individuation. Healthy, age-matched controls showed, on
404 average, a normalized Individuation Index of 1.00 (SD = 0.18). This refers to a slope of

405 0.087 (SD = 0.046), meaning that for a finger press of 10N the mean deviation of the
406 uninstructed fingers was 0.69N. As was the case for Strength, Individuation Indices in the
407 paretic hand were not correlated with age ($r = 0.16, p = 0.26$), nor affected by gender
408 ($t(51) = 0.17, p = 0.86$) or handedness ($t(51) = 0.34, p = 0.74$).

409 When introducing a new instrument, it is important to first establish its reliability,
410 i.e. the accuracy with which true inter-subject differences and intra-subject changes can
411 be determined. We therefore split the data for each session in half, calculated Strength
412 and Individuation Indices on these two independent data sets, and correlated the resultant
413 scores across patients and sessions (see Materials and Methods). The adjusted split-half
414 reliability across all patients and weeks for the Strength Index was $r_{full} = 0.99$ and 0.94 for
415 the paretic and non-paretic hands respectively, and $r_{full} = 0.89$ for controls, which
416 indicates good reliability. The adjusted split-half reliability of the Individuation Index of
417 all patients was $r_{full} = 0.99$ and 0.93 for the paretic and non-paretic hands respectively,
418 and for controls was $r_{full} = 0.97$.

419 Consistent with our effort to construct an individuation measure that is
420 independent of strength, the overall correlation between Individuation and Strength was
421 very low for controls ($r = -0.19, p = 0.51$).

422 ***The Strength and Individuation indices capture distinct aspects of standard clinical***
423 ***measures.***

424 We then compared the Strength and Individuation Indices with existing clinical
425 measures: the Fugl-Meyer (FM, a measure of impairment) and Action Reach Arm Test
426 (ARAT, a measure of activity). Table 2 shows the correlations for all four measures
427 obtained from the paretic hand across all time points. Overall, all correlations were high

428 (max $p = 1.21 \times 10^{-26}$), indicating that all the measures could detect severity of the hand
429 function deficit. The correlation in the patients between the two clinical measures was
430 0.91, whereas the correlation between the Strength and Individuation Indices was 0.73, a
431 significant difference ($z = 5.62, p = 2.0 \times 10^{-8}$, using Fisher's z -test (Fisher 1921) with $N =$
432 180; the total number of sessions for which both behavioral (Strength and Individuation
433 Indices) and clinical data (FM and ARAT) were available). Given comparable
434 reliabilities for all measures, this difference unlikely results from measurement noise –
435 rather it suggests that our Strength and Individuation Indices measure two different
436 aspects of the hand function, whereas the clinical scales tend to capture a mixture of
437 strength and control.

438 -----
439 Insert Table 1
440 -----

441 ***Recovery of strength and individuation occurred mainly in the first three months after***
442 ***stroke.***

443 We first examined the time courses of recovery for strength and individuation in
444 the paretic hand. If the two observed variables change in parallel, their recovery may or
445 may not be mediated by the same underlying process. A difference in the time courses,
446 however, would provide a strong hint of separate recovery processes for strength and
447 individuation.

448 For both measures, most of the recovery appeared to occur within the first 12
449 weeks after stroke (Fig. 2a-b). A mixed model with a fixed effect of Week and a random
450 effect of Subject was built to evaluate this statistically. An effect of Week was tested with

451 a likelihood ratio test against the null model with the random effect only. Results indicate
452 that both Strength and Individuation Indices significantly changed over time (Strength: χ^2
453 = 47.65, $p = 5.10 \times 10^{-12}$; Individuation: $\chi^2 = 18.58$, $p = 1.63 \times 10^{-5}$). Paired t -tests between
454 adjacent time points showed significant improvement (after Bonferroni correction) of the
455 Strength Index up to week 12; whereas the Individuation Index only showed a significant
456 improvement between weeks 4-12 (see detailed statistics in Fig. 2a-b). A similar recovery
457 curve was found for the standard clinical measures of motor function (detailed statistics
458 in Fig. 3).

459 To directly compare the time courses between the two indices at the early stage of
460 recovery, we z -normalized scores of the two variables and then investigated the change in
461 the scores for the time intervals W1-4 vs. W4-12 (Fig. 2c). This analysis suggests that
462 strength may recover mostly in the first four weeks, while individuation recovery may
463 occur equally in both time periods. Repeated-measures ANOVA over z -normalized
464 scores for Strength and Individuation Indices during the two time intervals yielded a
465 significant interaction ($F(1,25) = 6.82$, $p = 0.015$, Fig. 2c). Thus, despite overall
466 similarity, there was a significant difference in the time courses of recovery of strength
467 and individuation, with strength showing faster early recovery.

468 That most improvement in both strength and individuation occurred over the first
469 12 weeks can be observed not only in the mean recovery curve, but also in the variability
470 of inter-individual differences between adjacent testing time points (Fig. 2d). The
471 correlation between weeks 1 and 4 across individuals for the Individuation Index was
472 significantly lower than it was for subsequent time points (W1-4 vs. W24-52: $z = -4.23$,
473 $p = 2.3 \times 10^{-5}$), and this difference for Strength Index was marginally significant ($z = -$

474 1.83, $p = 0.067$), using z -test (Fisher 1921) with $N = 28$ and 33 . Thus, the relative
475 position of the patients on the mean recovery curve changed more during the first 4
476 weeks than during the last 6 months. This correlation difference cannot be attributed to
477 measurement noise, as both measures had high reliabilities at all time points (dashed
478 line). Instead, the lack of stability of these measures during early recovery is indicative of
479 meaningful biological change accelerating some patients' recovery, but not others.

480

481

Insert Figure 2

482

483 Consistent with previous findings (Noskin et al. 2008), the non-paretic hand also
484 showed mild impairment in the first month after stroke. A likelihood ratio test of the
485 mixed-effect model showed a significant effect of Week for Strength ($\chi^2 = 7.86$, $p =$
486 0.0051), and a more subtle effect for Individuation ($\chi^2 = 4.12$, $p = 0.042$) (Fig. 2a-b). This
487 increase in performance is unlikely to be related to a general practice effect, because the
488 Strength Index in healthy controls decreased slightly over time ($\chi^2 = 4.54$, $p = 0.033$),
489 perhaps due to reduced effort, whereas the Individuation Index for healthy controls was
490 maintained at a similar level over the whole year ($\chi^2 = 0.33$, $p = 0.56$). Thus, our results
491 confirmed previous finding that stroke appears to be associated with a mild ipsilateral
492 deficit in hand function (Noskin et al. 2008).

493 In summary, most recovery of both strength and individuation occurred in the first
494 three months after stroke, with stabilization of recovery around 3-6 months. The data also
495 suggest a slight difference in the time course, with strength recovering faster than
496 individuation in the first month.

497

498

Insert Figure 3

499

500 ***Evidence for a time-invariant relationship between strength and control.***

501 To examine the relationship between finger strength and control, we undertook a
502 closer examination of how the two variables relate to each other by plotting one against
503 the other at each testing time-point (Fig. 4a). Interestingly, the resultant function had a
504 distinct curvilinear shape that was preserved across weeks. At lower strength levels, there
505 was a clear correlation between strength and individuation; whereas once strength
506 recovered to above ~60% of normal levels, the two variables became uncoupled (Fig.
507 4b). Recovery was captured by a patient moving from the lower left corner to the upper
508 right corner of this function.

509 To formally test that the function's curvilinear shape is indeed time invariant, i.e.
510 it remains the same at all post-stroke time points, we first found a function to describe the
511 strength-individuation relationship. We used data from all time points and evaluated the
512 goodness of fit of a piecewise function with two linear segments connected at an
513 inflection point, using leave-one-out cross-validation (see Materials and Methods). Cross-
514 validation automatically penalizes models that are too complex. This functional form
515 gave us good prediction of the data (cross-validated $R^2 = 0.53$, Fig. 4b). We also explored
516 first- to fourth- order polynomial functions. All four models resulted in a worse
517 prediction than the piece-wise linear function (cross-validated $R^2 < 0.49$). We then tested
518 whether the function shape is the same across weeks. Using leave-one-out cross-
519 validation, the time-invariant model with fixed parameters across all weeks was

520 compared with a model allowing the parameters to change for each week (time-varying
521 model). The cross-validated R^2 for the time-varying two-segment piecewise linear
522 function was 0.45, a worse prediction than the time-invariant model.

523 These results suggest that there is indeed a time-invariant recovery relationship
524 between strength and individuation after stroke: up to a certain level of strength (60.7%
525 of non-paretic hand), Strength and Individuation Indices are strongly correlated ($r = 0.74$,
526 $p = 6.61 \times 10^{-18}$); after strength exceeds this threshold, the two variables are no longer
527 correlated ($r = -0.17$, $p = 0.11$; Fig 4b). This lack of correlation cannot be attributed to a
528 ceiling effect for the Individuation Index, because even above this level, the inter-subject
529 variances were still higher than the intra-subject variances in both patients and controls,
530 manifested as the high reliability of Individuation Index. This indicates that our measure
531 has enough dynamic range and sensitivity to detect inter-individual differences even in
532 the healthy population.

533 Overall, our results suggest that recovery can be captured as traversal along a
534 time-invariant function relating strength and individuation. Differences in recovery arise
535 because patients vary substantially in the distance they move along this function: some
536 patients with initial severe impairment made a good recovery, moving past the inflection
537 point of 60.7% strength (exemplified by the yellow dot in Fig. 4a). Other severely
538 impaired patients failed to reach the inflection point (red dot in Fig. 4a) (supplementary
539 video). Finally, some mildly impaired patients started off beyond the inflection point and
540 showed a good range of individuation recovery.

541

542

Insert Figure 4

543

544 *A second process contributed additional recovery of finger individuation.*

545 The fact that recovery of both strength and individuation could be captured by a
546 single time-invariant function that relates them is compatible with the hypothesis of a
547 single underlying process that drives recovery of both aspects of hand function. It is
548 possible, however, that an additional process injects further recovery, which determines a
549 patient's position relative to the mean recovery function. If such a process exists, a given
550 patient should occupy a consistent position above or below the mean recovery function
551 across time points. To test this hypothesis, we investigated the residuals of the
552 Individuation Index for each patient at each time point after subtracting the mean two-
553 segment piecewise-linear recovery function. If the variability around this mean function
554 were purely due to noise, we should observe no consistent week-by-week correlation
555 between residuals for each patient. Alternatively, if the residuals were to be correlated
556 across weeks, it would indicate that some patients were consistently better at
557 individuation than would be predicted by the function, and others were consistently
558 worse, suggesting an additional factor mediating individuation recovery (Fig. 5 black
559 arrows).

560 Correlations of residuals from adjacent time points across patients were initially
561 quite low. However, from week 4 onwards, most patients' distances from the mean
562 function remained stable (Fig. 4c-d). This consistent structure in residuals provides
563 evidence for an extra factor contributing to the recovery of individuation. The high
564 correlation of residuals at later time points could not be attributed to pre-morbid inter-
565 individual differences, because both Strength and Individuation Indices were normalized

566 to the non-paretic hand. The low week-by-week correlations between early time points
567 argue that the later correlations do not simply reflect sparing of a particular neural system
568 after stroke. If this had been true, correlation between the Individuation residuals should
569 have remained constant across all time points. Furthermore, the lower early correlation
570 cannot be attributed to measurement noise, as reliabilities for the early measurement
571 points were high (Fig. 4d). Rather, the initially low but then increasing correlation
572 indicates an additional recovery process operating above the lower bound of the strength-
573 individuation function (Fig. 5). This process is mostly active in the first three months
574 after stroke, and determines how well individuation recovers above that expected from
575 the time-invariant recovery function.

576

577

Insert Figure 5

578

579 ***Lesions involving the hand area of motor cortex and the corticospinal tract correlated***
580 ***more with individuation than strength.***

581 To investigate the underlying neural substrates of recovery processes, we
582 correlated the location and size of the lesion with the Strength and Individuation Indices.
583 Based on classic non-human primate studies (Lawrence and Kuypers 1968a, 1968b), we
584 predicted that individuation would integrally depend on the corticospinal tract (CST),
585 whereas strength may have contributions from other tracts, such as the reticulospinal tract
586 (RST). While cells originating from the RST also receive cortical input from the
587 precentral gyrus and are intermingled with the CST to some degree, cortical projections
588 to the reticular formation have a more widespread bilateral origin from other pre-motor

589 areas (Keizer and Kuypers 1989), whereas direct corticospinal projections to ventral horn
590 neurons primarily arise from the anterior bank of the precentral gyrus/central sulcus, i.e.
591 “new M1” (Rathelot and Strick 2009; Witham et al. 2016). We therefore predicted that
592 the extent of damage to the hand area of the primary motor cortex, and to the white
593 matter ROI that characterizes the most likely course of the CST (see Materials and
594 Methods) would correlate more with Individuation, and less with Strength. Furthermore,
595 lesions in these areas should correlate with individuation recovery over and above the
596 level expected from the mean recovery function.

597 As hypothesized, the extent of involvement by the lesion of the cortical hand area
598 correlated significantly with the Individuation Index at all time points. For the CST, all
599 correlations were significant after week 1 (Fig. 6b-c). While both lesion measures also
600 correlated with the Strength Index, these correlations were weaker (repeated-measures
601 ANOVA showed a significant main effect for behavioral measure ($F(1,3) = 146, p =$
602 0.001). This difference was not due to measurement noise, as Strength and Individuation
603 Indices had comparable reliabilities. Furthermore, percent lesion involvement also
604 significantly correlated with the Individuation Index, after accounting for the average
605 Strength-Individuation relationship ($p < 0.05$ for correlations after week 24 for cortical
606 hand area, and after week 12 for CST). Indeed, at W52, correlations with the residuals
607 were as high as with the Individuation Indices themselves ($r = 0.61$ vs. $r = 0.57$ for the
608 cortical hand area, $r = 0.51$ vs. $r = 0.54$ for the CST). Together these results suggest that
609 Individuation recovery is most heavily determined by sparing in the hand area of the
610 primary motor cortex and of CST projections, while strength recovery may also depend
611 on other spared descending pathways.

612

613

Insert Figure 6

614

615

Discussion

616

617

618

619

620

621

622

623

624

625

626

627

628

629

630

631

632

633

We tested patients at five time points over a one-year period after stroke, using a novel paradigm that separately measures maximum voluntary contraction force (a measure of strength) and finger individuation ability (a measure of control), and crucially controls for any obligatory dependency between these two measures. This approach allowed us to determine how recovery of strength and control interrelate. Our main question was to ask whether strength and control shared the same recovery mechanisms, after the two variables had been experimentally uncoupled. If they are truly dissociable, then hypothetically patients could show perfect control of individual fingers, even with significant weakness (except for complete hemiplegia, in which case no individuation measure would be obtainable). We showed that involuntary movements in uninstructed fingers (enslaving) increased with the level of force production of the instructed finger. This phenomenon is analogous to what Dewald and colleagues have described for the paretic arm (Sukal et al. 2007): loss of control, as indicated by a decrease in arm reaching workspace as the force requirement to resist gravity increases. Here we used the ratio of enslaved and instructed finger forces as an Individuation Index, thereby isolating the control component, and factoring out its dependence on force production. We show that this approach provides a sensitive measure of finger control independent of the level of force deficit.

634 Our paradigm quantifies two critical dimensions of hand function, as we argue
635 that real life actions such as precision grip involve a weighted combination of strength
636 and precision control of individual fingers (Xu et al. 2015). There are of course
637 limitations to this approach. Other dimensions, such as the use of tactile information from
638 the fingertips that are likely to be important for fine object manipulation, are not assessed
639 in our task. Furthermore, we assess individuation capability in a medium-to-high force
640 range (>20% MVF), while many fine motor actions demand lower levels of force. Note,
641 however, that 20% MVF for many patients corresponded to 5-10% MVF for healthy
642 controls in terms of absolute force, and therefore falls into the range of forces needed for
643 everyday fine-finger control actions. Overall, we think that our Strength and
644 Individuation Indices capture two fundamental aspects of hand function.

645 We first examined the time courses of recovery for strength and individuation.
646 Consistent with what has been described with traditional clinical scales (Duncan et al.
647 1992; Jørgensen et al. 1995; Krakauer et al. 2012), both measures showed that most
648 recovery occurred within the first three months after stroke. This similarity between the
649 time courses, however, does not necessarily imply that recovery of strength and
650 individuation is dependent on a single underlying neural substrate or mechanism. It
651 remains possible that recovery of these two components occurs in parallel because of
652 commonalities in basic tissue repair mechanisms post-ischemia, but they are nevertheless
653 independent modules. Indeed, we found a small but robust difference in the time course
654 of recovery of strength compared to control: finger strength showed a faster rate of
655 change compared to individuation over the first month.

656 Closer examination of the two variables revealed a time-invariant non-linear
657 relationship between strength and individuation in the paretic hand. This function has two
658 distinct parts: individuation and strength were highly correlated below a strength
659 threshold of ~60% of the non-paretic side; beyond this point, they were uncorrelated.

660 Recovery of hand function could be characterized as movement along the time-
661 invariant function (it had the same shape across all time points): patients with good
662 recovery traveled further along the function, whereas patients with poor recovery
663 remained in the first segment. The existence of the recovery function suggests that a
664 single system mediates recovery of both strength and individuation. This system can
665 generate strength but has only limited individuation capacity; beyond this threshold there
666 can be further increases in strength but no accompanying improvements in individuation.
667 It is important to note that the correlation at lower levels of strength recovery (<60%)
668 does *not* represent a causal relationship between strength and individuation, as by
669 definition the Individuation Index is corrected for strength. What this correlation at lower
670 strength level is capturing instead is a shared underlying recovery process, not an obligate
671 strength-control relationship. The lack of a causal relationship is also apparent in the fact
672 that some patients had a higher individuation index at relatively low levels of strength
673 (<60%), whereas others regained full strength but were still impaired with individuation
674 (Figure 4B).

675 Our analysis also revealed clear evidence for a second system that contributes to
676 recovery of individuation. There was systematic structure in the residuals around the
677 mean recovery function: patients at the chronic stages differed consistently in the amount
678 of individuation recovery they manifested relative to the level predicted by the recovery

679 function. Notably, their individuation relative to the mean recovery curve seemed to be
680 set early in the recovery process, and remained relatively stable at later time points. This
681 additional modulation of individuation implies a second recovery process adding to the
682 process represented by the mean recovery function.

683 Thus we propose that recovery of strength and individuation relies on partially
684 separable systems. One system contributes all of strength and some degree of
685 individuation. The isolated contribution of this system would determine the lower bound
686 of the data points in the strength-individuation plot (dashed line in Fig. 5): a patient
687 regains some strength and a limited amount of control. However, the amount of
688 individuation is limited and does not increase above a certain level. This would explain
689 both the strong correlation between strength and individuation for the severely impaired
690 patients, and the fact that no patient occupied the lower right corner of strength-
691 individuation space, i.e. no patients had good strength but minimal control. This recovery
692 principle may be applicable to effectors beyond the hand: we have recently demonstrated
693 a similar dissociation in strength and control for arm recovery in a subset of the same
694 cohort of patients (Cortes et al. 2017).

695 The second system would then add additional individuation (control capacity) to
696 the first system (vertical arrows in Fig. 5). Patients with a strong contribution from this
697 second system may gain full recovery of individuation; patients with no or only partial
698 contribution from the second system may recover strength completely but not
699 individuation. Importantly, the recovery of this second system also occurs early following
700 stroke, after which a patient's relative position above or below the mean recovery
701 function remains relatively fixed (Fig. 4d).

702 Lesion analysis adds support to the two-systems model for recovery suggested by
703 the behavioral data. A wealth of evidence in humans and non-human primates implicates
704 the role of CST in finger control, especially the monosynaptic cortico-motoneuronal
705 (CM) connections originating from “new” M1 (Rathelot and Strick 2006, 2009). Notably,
706 these connections do not generate high levels of force but rather finely graded forces
707 riding on top of larger forces (Maier et al. 1993). Consistent with this idea, lesions in the
708 gray matter of the hand areas in M1—the main origin of corticospinal projections—as
709 well as the CST, correlated more with impaired individuation than with strength. In
710 contrast, finger strength may rely on other neural pathways, including the RST, which
711 can support strength and gross movements (Buford and Davidson 2004; Davidson and
712 Buford 2004). Although the RST has been found to participate in some degree of finger
713 control, its functional range is limited and biased towards flexor muscles (Riddle et al.
714 2009; Baker 2011).

715 Recovery after stroke is likely to result from the dynamic interplay between the
716 CST and other descending pathways, particularly the RST. In this scenario, the
717 correlation between strength and control at low levels of strength may represent the state
718 of both the residual CST and of cortical projections to reticular nuclei in the brainstem. In
719 contrast, recovery along the lower bound of the invariant function would represent the
720 contribution of the RST and other non-CST descending pathways, as strengthening of
721 RST connections to motoneurons has been shown in monkeys with CST lesions (Zaaimi
722 et al. 2012). Those patients with less damage to the CST would consistently ride above
723 this function, reflecting better individuation ability. While the origin of the
724 corticoreticular inputs is more diffuse (Keizer and Kuypers 1989) and bi-laterally

725 organized (Buford and Davidson 2004; Sakai et al. 2009; Soteropoulos et al. 2012), many
726 projections to the reticular formation arise from the “old” M1 (Catsman-Berrevoets and
727 Kuypers 1976; Jones and Wise 1977). Our CST and hand M1 lesion ROIs, despite our
728 best efforts, will have certainly been contaminated to some degree by non-CST fibers,
729 including the corticoreticular tract and other corticofugal fibers synapsing in the brain
730 stem. These additional descending pathways could in part explain the lower but
731 nevertheless significant correlation with strength.

732 In summary, we show with a novel behavioral paradigm and analysis that
733 recovery of hand function reflects the interplay between two independent systems. One
734 contributes strength and some degree of fine motor control. The second system then
735 provides additional fine motor control.

736

Acknowledgement

737 We thank Adrian Haith and Martin Lindquist for helpful discussions about data analysis.

738

739

Grants

740 This main study was supported by James S. McDonnell Foundation JMSF 90043345 and

741 220020220. Additional support came from a Scholar Award from the James S.

742 McDonnell Foundation and a Grant from the Wellcome Trust (094874/Z/10/Z) to Jörn

743 Diedrichsen. Andreas R. Luft is supported by the P&K Pühringer Foundation.

744

References

- 745 **Baker SN.** The primate reticulospinal tract, hand function and functional recovery. *J*
746 *Physiol* 589: 5603–5612, 2011.
- 747 **Bates D, Mächler M, Bolker B, Walker S.** Fitting Linear Mixed-Effects Models using
748 lme4. *ArXiv14065823 Stat.*
- 749 **Brainard DH.** The Psychophysics Toolbox. *Spat Vis* 10: 433–436, 1997.
- 750 **Buford JA, Davidson AG.** Movement-related and preparatory activity in the
751 reticulospinal system of the monkey. *Exp Brain Res* 159: 284–300, 2004.
- 752 **Catsman-Berrevoets CE, Kuypers HG.** Cells of origin of cortical projections to dorsal
753 column nuclei, spinal cord and bulbar medial reticular formation in the rhesus monkey.
754 *Neurosci Lett* 3: 245–252, 1976.
- 755 **Ceritoglu C, Oishi K, Li X, Chou M-C, Younes L, Albert M, Lyketsos C, van Zijl**
756 **PCM, Miller MI, Mori S.** Multi-contrast large deformation diffeomorphic metric
757 mapping for diffusion tensor imaging. *NeuroImage* 47: 618–627, 2009.
- 758 **Colebatch JG, Gandevia SC.** The Distribution of Muscular Weakness in Upper Motor
759 Neuron Lesions Affecting the Arm. *Brain* 112: 749–763, 1989.
- 760 **Connolly K, Elliott J.** The evolution and ontogeny of hand function. In: *Ethological*
761 *studies of child behaviour.* Oxford, England: Cambridge U. Press, 1972, p. x, 400.
- 762 **Cortes JC, Goldsmith J, Harran MD, Xu J, Kim N, Schambra HM, Luft AR, Celnik**
763 **P, Krakauer JW, Kitago T.** A Short and Distinct Time Window for Recovery of Arm
764 Motor Control Early After Stroke Revealed With a Global Measure of Trajectory
765 Kinematics. *Neurorehabil Neural Repair* 31: 552–560, 2017.

766 **Dale AM, Fischl B, Sereno MI.** Cortical surface-based analysis. I. Segmentation and
767 surface reconstruction. *NeuroImage* 9: 179–194, 1999.

768 **Davidson AG, Buford JA.** Motor outputs from the primate reticular formation to
769 shoulder muscles as revealed by stimulus-triggered averaging. *J Neurophysiol* 92: 83–95,
770 2004.

771 **Duncan PW, Goldstein LB, Matchar D, Divine GW, Feussner J.** Measurement of
772 motor recovery after stroke. Outcome assessment and sample size requirements. *Stroke J*
773 *Cereb Circ* 23: 1084–1089, 1992.

774 **Fischl B, Rajendran N, Busa E, Augustinack J, Hinds O, Yeo BTT, Mohlberg H,**
775 **Amunts K, Zilles K.** Cortical folding patterns and predicting cytoarchitecture. *Cereb*
776 *Cortex N Y N 1991* 18: 1973–1980, 2008.

777 **Fisher RA.** On the “Probable Error” of a coefficient of correlation deduced from a small
778 sample. *Metron* : 1–32, 1921.

779 **Fugl-Meyer AR, Jääskö L, Leyman I, Steglind S.** The post-stroke hemiplegic patient.
780 1. a method for evaluation of physical performance. *Scand J Rehabil Med* 7: 13–31,
781 1975.

782 **Guttman L.** A basis for analyzing test-retest reliability. *Psychometrika* 10: 255–282,
783 1945.

784 **Heller A, Wade DT, Wood VA, Sunderland A, Hewer RL, Ward E.** Arm function
785 after stroke: measurement and recovery over the first three months. *J Neurol Neurosurg*
786 *Psychiatry* 50: 714–719, 1987.

787 **Holland PW, Welsch RE.** Robust regression using iteratively reweighted least-squares.
788 *Commun Stat - Theory Methods* 6: 813–827, 1977.

789 **Jones EG, Wise SP.** Size, laminar and columnar distribution of efferent cells in the
790 sensory-motor cortex of monkeys. *J Comp Neurol* 175: 391–438, 1977.

791 **Jørgensen HS, Nakayama H, Raaschou HO, Vive-Larsen J, Støier M, Olsen TS.**
792 Outcome and time course of recovery in stroke. Part II: Time course of recovery. The
793 copenhagen stroke study. *Arch Phys Med Rehabil* 76: 406–412, 1995.

794 **Kamper DG, Harvey RL, Suresh S, Rymer WZ.** Relative contributions of neural
795 mechanisms versus muscle mechanics in promoting finger extension deficits following
796 stroke. *Muscle Nerve* 28: 309–318, 2003.

797 **Kamper DG, Rymer WZ.** Impairment of voluntary control of finger motion following
798 stroke: role of inappropriate muscle coactivation. *Muscle Nerve* 24: 673–681, 2001.

799 **Keizer K, Kuypers HG.** Distribution of corticospinal neurons with collaterals to the
800 lower brain stem reticular formation in monkey (*Macaca fascicularis*). *Exp Brain Res* 74:
801 311–318, 1989.

802 **Krakauer JW, Carmichael ST, Corbett D, Wittenberg GF.** Getting
803 neurorehabilitation right: what can be learned from animal models? *Neurorehabil Neural*
804 *Repair* 26: 923–931, 2012.

805 **Laird NM, Ware JH.** Random-effects models for longitudinal data. *Biometrics* 38: 963–
806 974, 1982.

807 **Lang CE, Schieber MH.** Differential impairment of individuated finger movements in
808 humans after damage to the motor cortex or the corticospinal tract. *J Neurophysiol* 90:
809 1160–1170, 2003.

810 **Lang CE, Schieber MH.** Reduced muscle selectivity during individuated finger
811 movements in humans after damage to the motor cortex or corticospinal tract. *J*
812 *Neurophysiol* 91: 1722–1733, 2004.

813 **Lawrence DG, Kuypers HG.** The functional organization of the motor system in the
814 monkey. II. The effects of lesions of the descending brain-stem pathways. *Brain J Neurol*
815 91: 15–36, 1968a.

816 **Lawrence DG, Kuypers HG.** The functional organization of the motor system in the
817 monkey. I. The effects of bilateral pyramidal lesions. *Brain J Neurol* 91: 1–14, 1968b.

818 **Leigh R, Oishi K, Hsu J, Lindquist M, Gottesman RF, Jarso S, Crainiceanu C, Mori**
819 **S, Hillis AE.** Acute lesions that impair affective empathy. *Brain J Neurol* 136: 2539–
820 2549, 2013.

821 **Li S, Latash ML, Yue GH, Siemionow V, Sahgal V.** The effects of stroke and age on
822 finger interaction in multi-finger force production tasks. *Clin Neurophysiol Off J Int Fed*
823 *Clin Neurophysiol* 114: 1646–1655, 2003.

824 **Li ZM, Latash ML, Zatsiorsky VM.** Force sharing among fingers as a model of the
825 redundancy problem. *Exp Brain Res* 119: 276–286, 1998.

826 **Lyle RC.** A performance test for assessment of upper limb function in physical
827 rehabilitation treatment and research. *Int J Rehabil Res Int Z Rehabil Rev Int Rech*
828 *Readaptation* 4: 483–492, 1981.

829 **Maier MA, Bennett KM, Hepp-Reymond MC, Lemon RN.** Contribution of the
830 monkey corticomotoneuronal system to the control of force in precision grip. *J*
831 *Neurophysiol* 69: 772–785, 1993.

832 **Mori S, Oishi K, Jiang H, Jiang L, Li X, Akhter K, Hua K, Faria AV, Mahmood A,**
833 **Woods R, Toga AW, Pike GB, Neto PR, Evans A, Zhang J, Huang H, Miller MI,**
834 **van Zijl P, Mazziotta J.** Stereotaxic white matter atlas based on diffusion tensor imaging
835 in an ICBM template. *NeuroImage* 40: 570–582, 2008.

836 **Mori S, Wakana S, Nague-Poetscher LM, Van Zijl PCM.** MRI Atlas of Human White
837 Matter Elsevier. *Amst. Neth.*

838 **Napier JR.** The prehensile movements of the human hand. *J Bone Joint Surg Br* 38–B:
839 902–913, 1956.

840 **Noskin O, Krakauer JW, Lazar RM, Festa JR, Handy C, O’Brien KA, Marshall RS.**
841 Ipsilateral motor dysfunction from unilateral stroke: implications for the functional
842 neuroanatomy of hemiparesis. *J Neurol Neurosurg Psychiatry* 79: 401–406, 2008.

843 **Oishi K, Faria AV, van Zijl PC, Mori S.** MRI atlas of human white matter. Academic
844 Press.

845 **Oishi K, Zilles K, Amunts K, Faria A, Jiang H, Li X, Akhter K, Hua K, Woods R,**
846 **Toga AW, Pike GB, Rosa-Neto P, Evans A, Zhang J, Huang H, Miller MI, van Zijl**
847 **PCM, Mazziotta J, Mori S.** Human brain white matter atlas: identification and
848 assignment of common anatomical structures in superficial white matter. *NeuroImage* 43:
849 447–457, 2008.

850 **Oldfield RC.** The assessment and analysis of handedness: the Edinburgh inventory.
851 *Neuropsychologia* 9: 97–113, 1971.

852 **Picard RR, Cook RD.** Cross-Validation of Regression Models. *J Am Stat Assoc* 79:
853 575–583, 1984.

854 **Rathelot J-A, Strick PL.** Muscle representation in the macaque motor cortex: an
855 anatomical perspective. *Proc Natl Acad Sci U S A* 103: 8257–8262, 2006.

856 **Rathelot J-A, Strick PL.** Subdivisions of primary motor cortex based on cortico-
857 motoneuronal cells. *Proc Natl Acad Sci* 106: 918–923, 2009.

858 **Reinkensmeyer DJ, Lum PS, Lehman SL.** Human control of a simple two-hand grasp.
859 *Biol Cybern* 67: 553–564, 1992.

860 **Riddle CN, Edgley SA, Baker SN.** Direct and indirect connections with upper limb
861 motoneurons from the primate reticulospinal tract. *J Neurosci Off J Soc Neurosci* 29:
862 4993–4999, 2009.

863 **Sakai ST, Davidson AG, Buford JA.** Reticulospinal neurons in the pontomedullary
864 reticular formation of the monkey (*Macaca fascicularis*). *Neuroscience* 163: 1158–1170,
865 2009.

866 **Schieber MH.** Individuated finger movements of rhesus monkeys: a means of
867 quantifying the independence of the digits. *J Neurophysiol* 65: 1381–1391, 1991.

868 **Soteropoulos DS, Williams ER, Baker SN.** Cells in the monkey ponto-medullary
869 reticular formation modulate their activity with slow finger movements. *J Physiol* 590:
870 4011–4027, 2012.

871 **Sukal TM, Ellis MD, Dewald JPA.** Shoulder abduction-induced reductions in reaching
872 work area following hemiparetic stroke: neuroscientific implications. *Exp Brain Res* 183:
873 215–223, 2007.

874 **Sunderland A, Tinson D, Bradley L, Hewer RL.** Arm function after stroke. An
875 evaluation of grip strength as a measure of recovery and a prognostic indicator. *J Neurol*
876 *Neurosurg Psychiatry* 52: 1267–1272, 1989.

877 **Wakana S, Caprihan A, Panzenboeck MM, Fallon JH, Perry M, Gollub RL, Hua K,**
878 **Zhang J, Jiang H, Dubey P, Blitz A, van Zijl P, Mori S.** Reproducibility of
879 quantitative tractography methods applied to cerebral white matter. *NeuroImage* 36: 630–
880 644, 2007.

881 **Witham CL, Fisher KM, Edgley SA, Baker SN.** Corticospinal Inputs to Primate
882 Motoneurons Innervating the Forelimb from Two Divisions of Primary Motor Cortex and
883 Area 3a. *J Neurosci Off J Soc Neurosci* 36: 2605–2616, 2016.

884 **Xu J, Haith AM, Krakauer JW.** Motor Control of the Hand Before and After Stroke.
885 In: *Clinical Systems Neuroscience*. Springer, p. 271–289.

886 **Yousry TA, Schmid UD, Alkadhi H, Schmidt D, Peraud A, Buettner A, Winkler P.**
887 Localization of the motor hand area to a knob on the precentral gyrus. A new landmark.
888 *Brain J Neurol* 120 (Pt 1): 141–157, 1997.

889 **Zaaimi B, Edgley SA, Soteropoulos DS, Baker SN.** Changes in descending motor
890 pathway connectivity after corticospinal tract lesion in macaque monkey. *Brain J Neurol*
891 135: 2277–2289, 2012.

892 **Zatsiorsky VM, Li ZM, Latash ML.** Enslaving effects in multi-finger force production.
893 *Exp Brain Res* 131: 187–195, 2000.

894 **Zhang W, Olivi A, Hertig SJ, van Zijl P, Mori S.** Automated fiber tracking of human
895 brain white matter using diffusion tensor imaging. *NeuroImage* 42: 771–777, 2008.

896 **Zhang Y, Zhang J, Oishi K, Faria AV, Jiang H, Li X, Akhter K, Rosa-Neto P, Pike**
897 **GB, Evans A, Toga AW, Woods R, Mazziotta JC, Miller MI, van Zijl PCM, Mori S.**
898 Atlas-guided tract reconstruction for automated and comprehensive examination of the
899 white matter anatomy. *NeuroImage* 52: 1289–1301, 2010.

900 **Figure 1.** *Strength and Individuation task. Fifty-four patients and 14 healthy controls*
901 *were tested five times over one-year period. (a) Ergonomic hand device. Force*
902 *transducers beneath each key measured the force exerted by each finger in real time. The*
903 *participant's fingers are securely placed on the keys using Velcro straps. (b) Computer*
904 *screen showing the instructional stimulus, which indicates both which finger to press and*
905 *how much force to produce (height of the green bar). In the MVF task, maximal force*
906 *was required. MVF trials were performed twice on each finger. In the Individuation task,*
907 *one of four target force levels had to be reached. Target force levels were 20, 40, 60, and*
908 *80% of MVF for each digit. Individuation trials were performed four times per force level*
909 *per digit. (c, d) Example trials from two healthy control participants during the*
910 *Individuation task. Four trials are shown, one at 20% and one at 80% of MVF for the*
911 *two participants. In this case the fourth finger (red) was the instructed finger. Note the*
912 *higher level of enslaving of the uninstructed fingers for higher instructed finger force*
913 *level. (e) Mean deviation from baseline in the uninstructed fingers plotted against the*
914 *force generated by the instructed finger for (c) and (d). The Individuation Index is the -*
915 *log(slope) of the regression line between instructed finger force and uninstructed mean*
916 *deviation, measured as root mean square (RMS) force from baseline force produced by*
917 *uninstructed fingers. (f, g) Example trials from one patient during the Individuation task,*
918 *two from each time point over the one-year period: at 40% (f) and 80% (g) MVF.*
919 *Instructed finger for each trial was the same as those shown in control data (c, d). (h)*
920 *Force-control trade-off function at each time point for the example patients, showing*
921 *higher level of enslaving early after stroke, and recovery of individuation ability over*
922 *time.*

923

924 **Figure 2.** Temporal profiles of recovery for strength and individuation. **(a-b)** Group
925 recovery curves for the Strength and Individuation Indices for patients and controls.
926 Asterisks indicate significant week-to-week change for the paretic hand (Bonferroni
927 corrected p-values for each segments of Strength Index: $p(W1-4) = 0.0045$, $p(W4-12) =$
928 0.0082 , $p(W12-24) = 0.068$, $p(W24-52) = 0.87$; Individuation Index: : $p(W1-4) = 0.81$,
929 $p(W4-12) = 0.0024$, $p(W12-24) = 1.92$, $p(W24-52) = 2.91$). **(c)** Rate of change (i.e.,
930 change per week) in Z-normalized Strength and Individuation Indices during the first two
931 intervals (Week 1 to 4 and Week 4 to 12). The two intervals show a significant interaction
932 between strength and individuation, indicating faster initial improvement of strength; **(d)**
933 Week-to-week correlations between adjacent time points for the Strength and
934 Individuation Indices. Dashed lines are the noise ceilings based on the within-session
935 split-half reliabilities. (Sample size $N = 53$ patients, 14 controls, with a total of 251
936 completed sessions.)

937

938 **Figure 3.** Temporal recovery profiles measures with clinical assessments. **(a)** Fugl-
939 Meyer for the arm (FM-Arm) and **(b)** hand (FM-Hand); **(c)** ARAT. All measures showed
940 significant change over time for the paretic hand. FM-Arm: $\chi^2 = 37.73$, $p = 8.13 \times 10^{-10}$;
941 FM-Hand: $\chi^2 = 29.03$, $p = 7.14 \times 10^{-8}$; ARAT: $\chi^2 = 36.33$, $p = 1.67 \times 10^{-9}$. (Sample size $N =$
942 53 patients, 14 controls, with total completed sessions for FM and ARAT were 238 and
943 235 respectively.)

944

945 **Figure 4.** Time-invariant impairment function relating strength and control. (a) Scatter
946 plots for Individuation against Strength Indices at each time point. Each black dot is one
947 patient's data; blue dots and ellipse indicates the mean and standard error for controls at
948 the time point. Two patients' data are highlighted: one with good recovery (yellow dot)
949 and one with poor recovery (red dot). Total number of patients at each time points are:
950 39, 39, 40, 39, and 34 for W1-52, respectively. (b) Scatter plot with data from all time
951 points superimposed with the best fitting two-segment piecewise-linear function with one
952 inflection point at Strength Index = 0.607. (c) Residuals from each week subtracting out
953 the mean impairment function (b, red line). The tendency of the residuals to stay above or
954 below the typical Strength-Individuation relationship indicates that there are stable
955 factors that determine Individuation recovery over and above strength recovery. (d)
956 Correlations of residuals from (c) across adjacent time points increased over time
957 (Bonferroni corrected $p(W1-4) = 2.12$, $p(W4-12) = 0.00064$, $p(W12-24) = 0.0024$,
958 $p(W24-52) = p = 3.39 \times 10^{-6}$). Dashed line is the noise ceilings based on the within-
959 session split-half reliabilities. (Sample size $N = 53$ patients, 14 controls, with a total of
960 251 completed sessions.)

961

962 **Figure 5.** A schematic diagram of the hypothesis of two recovery systems. The first
963 system (basic strength recovery) underlies strength recovery and a restricted amount of
964 individuation recovery. This system therefore defines the lower bound (dashed line) of the
965 space occupied by recovering patients (gray cloud). A second system (additional
966 individuation recovery) adds further individuation abilities on top of the basic strength
967 recovery.

968

969 **Figure 6.** *Lesion distribution and correlation with behavior. (a) Averaged lesion*
970 *distribution mapped to JHU-MNI space (see Materials and Methods), with lesion flipped*
971 *to one hemisphere. Color bar indicates patient count. (b) Correlation of behavior*
972 *measures (Strength and Individuation Indices) at each time point with the percentage of*
973 *damaged cortical gray matter within the M1 hand area ROI, corticospinal tract (CST).*
974 *Black asterisks indicate significant correlations (tested against zero), and red asterisks*
975 *indicate a significant difference between the correlation for Strength and Individuation*
976 *for each week ($p < 0.005$). (c) Mean of week-by-week correlations between the two*
977 *behavior measures and percent lesion volume measures for the cortical gray matter hand*
978 *area and CST ROI. (Sample size $N = 53$, with 251 completed sessions.)*

979 **Table 1.** Patient characteristics: age (years), sex, paretic side, initial FM-Arm (Fugl-
980 Meyer arm score, maximum 66), initial MoCA (Montreal Cognitive Assessment,
981 maximum 30).

982

| Patient | Age at stroke | Gender | Paretic Side | Initial impairment (FM-Arm) | Initial MoCA | SRI |
|---------|---------------|--------|--------------|-----------------------------|--------------|--------------|
| 1 | 57 | M | R | 48 | 27 | No |
| 2 | 24 | M | L | 35 | 23 | No |
| 3 | 67 | F | R | 16 | 23 | Fluoxetine |
| 4 | 74 | F | R | 39 | 17 | No |
| 5 | 61 | F | L | 48 | 26 | No |
| 6 | 59 | F | R | 60 | 28 | Sertraline |
| 7 | 57 | M | R | 54 | 27 | No |
| 8 | 66 | M | L | 65 | 25 | No |
| 9 | 42 | F | R | 5 | 18 | No |
| 10 | 65 | M | L | 30 | 25 | No |
| 11 | 66 | F | L | 60 | 19 | Fluoxetine |
| 12 | 51 | M | L | 34 | 25 | No |
| 13 | 63 | F | L | 57 | 26 | No |
| 14 | 55 | M | L | 0 | 26 | Fluoxetine |
| 15 | 56 | M | L | 38 | 25 | Fluoxetine |
| 16 | 56 | M | L | 64 | 24 | No |
| 17 | 64 | F | R | 20 | 16 | Trazodone |
| 18 | 60 | F | R | 55 | 21 | Fluoxetine |
| 19 | 64 | M | L | 63 | 25 | Fluoxetine |
| 20 | 25 | F | L | 42 | 29 | Fluoxetine |
| 21 | 39 | F | L | 47 | 20 | Fluoxetine |
| 22 | 46 | M | L | 9 | 27 | Fluoxetine |
| 23 | 53 | F | L | 4 | 29 | No |
| 24 | 66 | M | L | 59 | 24 | Escitalopram |
| 25 | 71 | M | L | 4 | 26 | No |
| 26 | 52 | M | L | 53 | 24 | No |
| 27 | 46 | M | R | 4 | 21 | Trazodone |
| 28 | 46 | M | L | 49 | 30 | No |
| 29 | 71 | M | L | 6 | 24 | No |
| 30 | 47 | M | R | 57 | 10 | No |
| 31 | 45 | M | L | 8 | 27 | No |
| 32 | 55 | F | L | 19 | 25 | Escitalopram |
| 33 | 68 | F | L | 61 | NaN | Escitalopram |
| 34 | 65 | M | L | 32 | 28 | No |
| 35 | 51 | F | L | 63 | 26 | Escitalopram |
| 36 | 42 | M | R | 54 | 25 | No |
| 37 | 58 | M | L | 4 | 24 | No |
| 38 | 41 | F | L | 4 | 23 | No |
| 39 | 35 | M | L | 4 | 29 | Escitalopram |
| 40 | 68 | M | L | 52 | 27 | Escitalopram |
| 41 | 76 | M | L | 53 | 18 | Sertraline |

| | | | | | | |
|----|----|---|---|----|----|--------------|
| 42 | 86 | M | L | 54 | 20 | Escitalopram |
| 43 | 48 | M | L | 16 | 25 | No |
| 44 | 74 | M | R | 5 | 25 | No |
| 45 | 80 | F | R | 9 | 24 | No |
| 46 | 64 | F | L | 58 | 19 | No |
| 47 | 22 | M | R | 63 | 27 | No |
| 48 | 88 | F | R | 55 | 28 | No |
| 49 | 22 | M | R | 63 | 27 | No |
| 50 | 87 | F | R | 50 | 28 | No |
| 51 | 84 | M | R | 30 | 26 | Escitalopram |
| 52 | 53 | M | R | 30 | 29 | No |
| 53 | 54 | M | L | 59 | 21 | No |
| 54 | 58 | M | R | 61 | 23 | No |

983

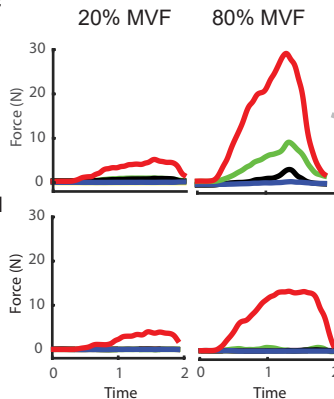
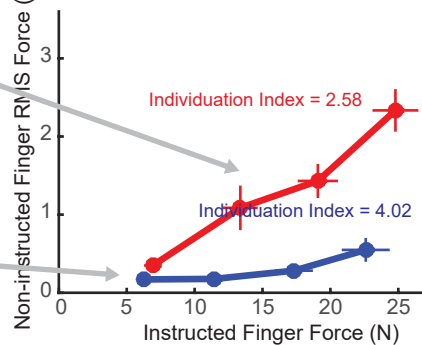
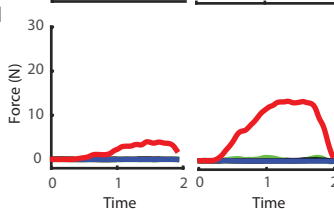
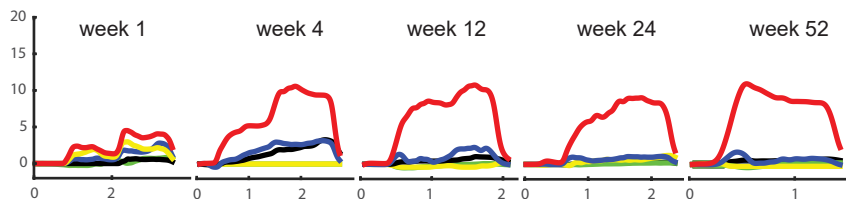
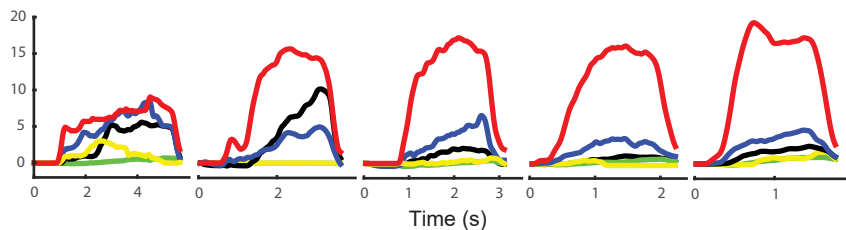
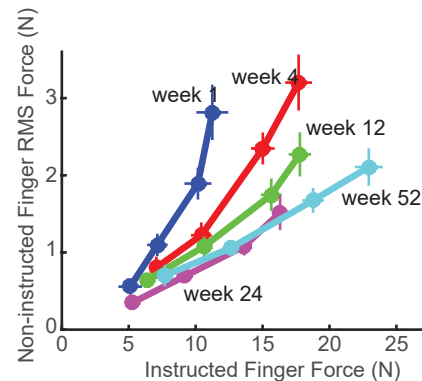
984 **Table 2.** *Correlation between Strength Index, Individuation Index, FM-Arm (Fugl-Meyer*
 985 *arm score, maximum 66), and ARAT (Action Reach Arm Test, maximum 57). All four*
 986 *measures are highly correlated; however Strength and Individuation Indices show the*
 987 *weaker correlation compared to that between FM-Arm and ARAT.*

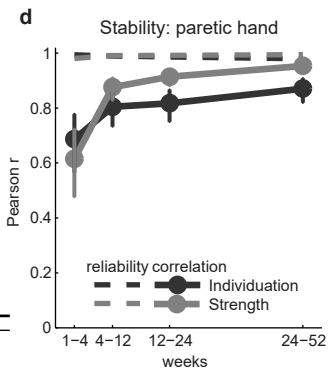
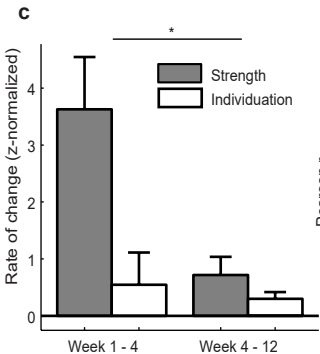
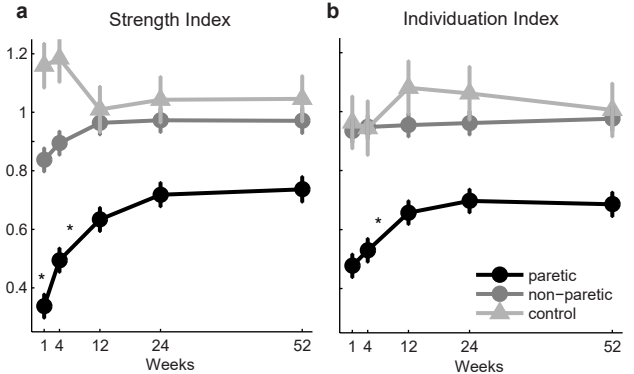
988

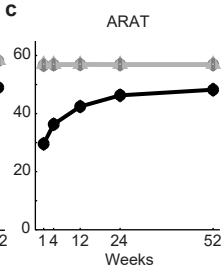
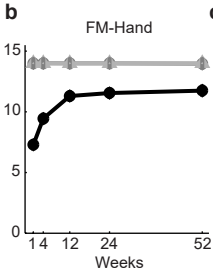
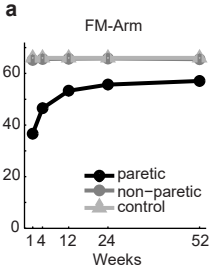
| | Strength Index | Individuation Index | FM-Arm | ARAT |
|---------------------|----------------|---------------------|--------|------|
| Strength Index | | 0.73 | 0.76 | 0.74 |
| Individuation Index | | | 0.68 | 0.72 |
| FM-Arm | | | | 0.91 |

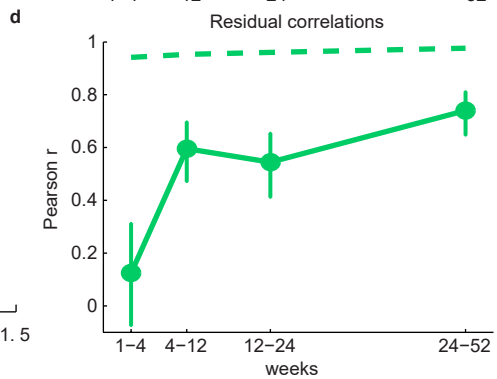
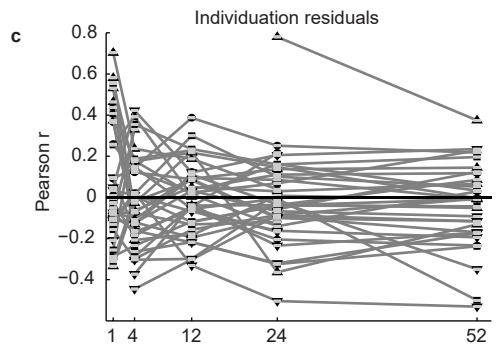
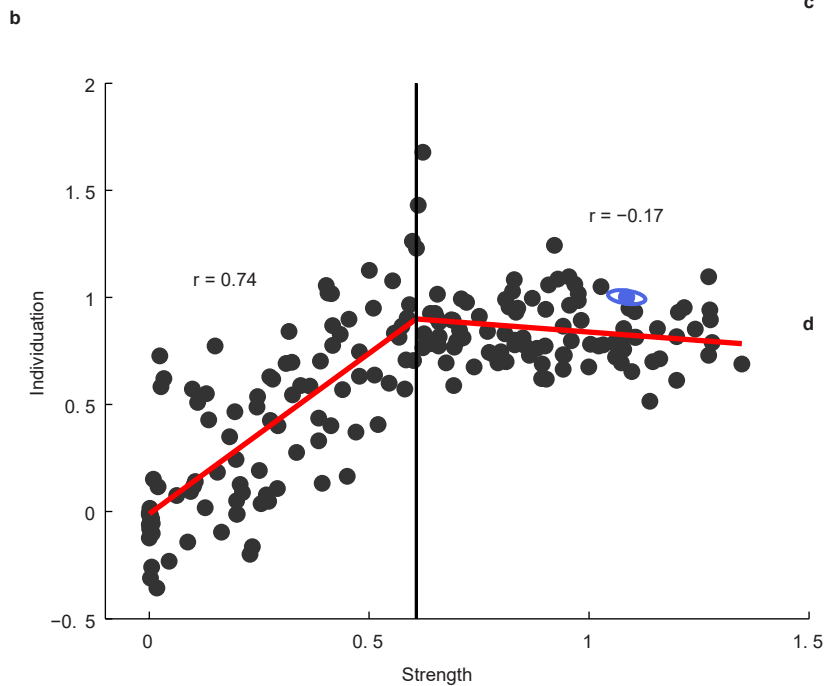
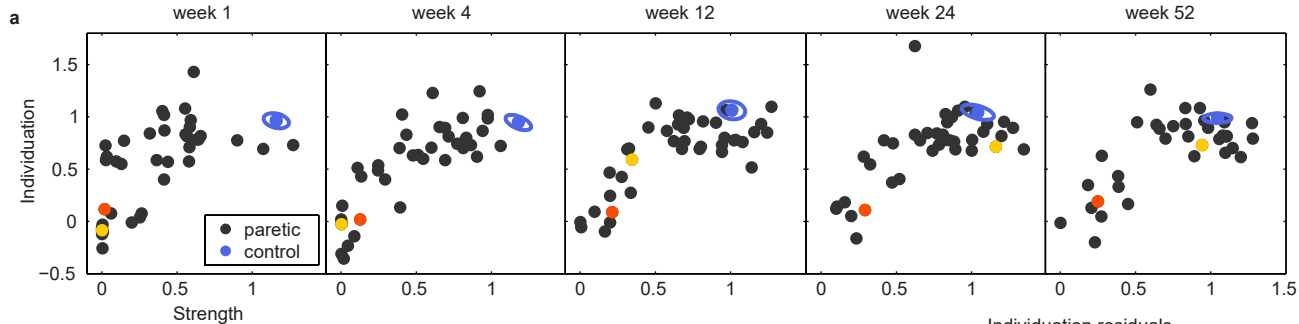
989

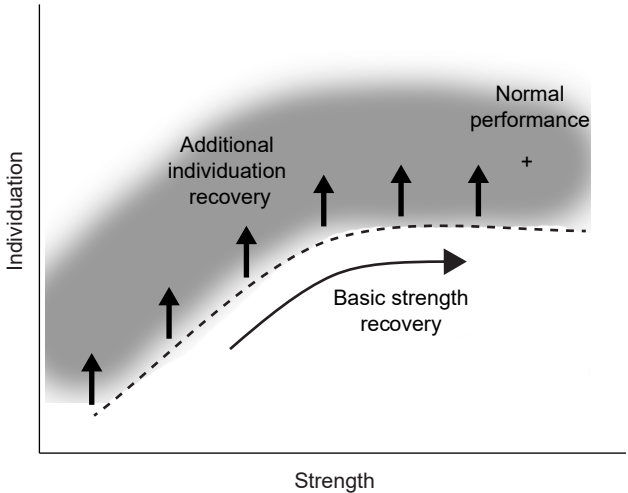
990 **Supplementary Video 1.** Migration of patients Strength and Individuation recovery along
991 the time-invariant function, over one year period after stroke. Each dot represents one
992 patient's position in the Strength-Individuation space. Thirty-four patients who finished
993 more than 3 time points were shown. Movement trajectories for each data point were
994 generated by fitting all the available data points for each patient using smoothing spline
995 function, weighted by group means, and with smoothing parameter 0.3. Strength and
996 Individuation trajectories were fit separately. For each movie frame, data for each
997 patient were drawn from the fitted spline function for the specific time slice. The two-
998 segment red line represents the time-invariant function, calculated from all the available
999 real data (see Methods). Note that at any time during recovery, all patients' recovery
1000 trajectories were largely following the curve-linear shaped mean recovery function. Two
1001 patients' trajectories are highlighted: one with good recovery that traversed the entire
1002 time-invariant function (yellow dot), and one with poor recovery that lingered around the
1003 lower-left corner of the mean recovery function (red dot).

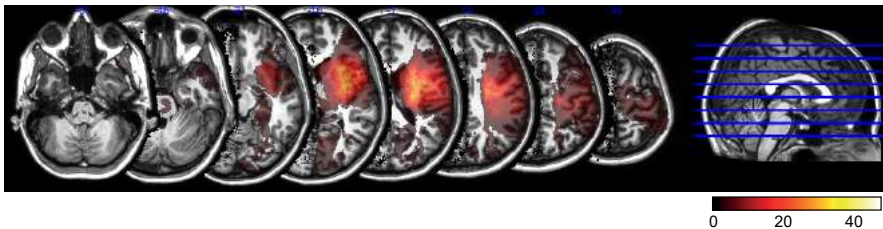
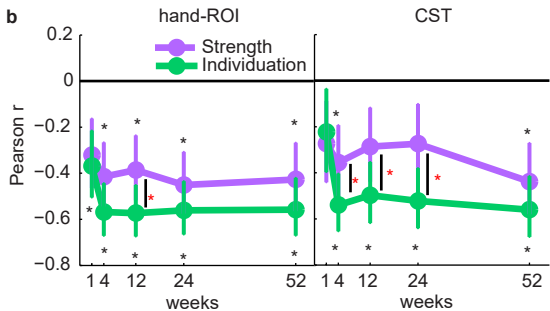
a**c****e****b****d****f** 40% MVF**g** 80% MVF**h**









a**b****c**